Influence of contact parameters in fretting-fatigue contact 3D problems

Fella Hamadouche, Habib Benzaama, Mohamed Mokhtari

Laboratory of Biomechanics and Biomaterials, National Polytechnic School of Oran ENPO, Algeria
fella.ham@hotmail.fr ,http://orcid.org/0000-0002-5306-0336
Habib.benzaama@enp-oran, mokhtarimohamed44@yahoo.fr

Miloud Abbes Tahar

Laboratory of Mechanical and Energy, University of Hassiba Benbouali, chlef, Algeria
taharabbes@yahoo.fr

ABSTRACT. A numerical study on the influence of contact parameters on fretting fatigue behavior is carried out by using a new method SFEM (Stretching Finite Element Method) is presented in this article. Several parameters are made to vary: geometric shapes of the mesh, materials and contact parameters. The three-dimensional parametric model is composed by specimen and a pad in full contact. A Fortran Code is used to generate the parametric mesh. The stress intensity factors are calculated by varying the above contact parameters and the stress intensity factor under modes 1, 2 and 3 are computed.

KEYWORDS. Fretting fatigue; Finite Element Method; 3 dimensions; crack and the stress intensity factors.

INTRODUCTION

Fretting occurs when two bodies are in contact, where a load presses these two bodies together [1]. A damage process is created between them. Fatigue is a phenomenon that occurs when a metal component is subjected to variable loads over time and after a given number of loading, a crack can initiate and grow until the component reaches breaking point [2]. Fatigue can occur when there are parts in contact, called fretting fatigue [2]. This phenomenon may occur in several mechanical connections such as the turbines, bearing; steel cables etc. Fretting fatigue can reduce the lifetime of a component compared with plane fatigue [4]. Many researchers use the fretting fatigue models to understand the details of fretting fatigue and to classify the importance of the design parameters involved in this phenomenon [5]. In recent years, a major effort has been made to study the phenomenon of fretting fatigue. Nowell et al. [6] describes a series of fretting fatigue experiments carried out under closely controlled conditions of partial slip. Ochi et al. [7] investigated the effect of contact pressure and slip amplitude on fretting fatigue behaviour of rail steel with fishplate: the results shows that the fretting fatigue strength decrease with increasing the contact pressure and the pad length. Tesh et al. [8] investigated the titanium alloy Ti-6Al-4V behaviour in fretting fatigue using a sphere on flat contact, to study the influence of microstructure and

contact condition. Kond et al. [9] proposed a local stress concept to evaluate the fretting fatigue limit for contact edge cracks. Ciavarella et al. [10] solved the contact problem compared with plain of fatigue for a flat punch having rounded corners under condition of normal loading and a shearing force. Heung et al. [11] proposed hybrid layer method to examine the effect of finite width of contact finite on fretting fatigue according to this method traction distribution obtained from the coarse finite element three-dimensional analyses was used in two-dimensional plane strain finite element model to increase computational efficiency. Kataoka et al. [12] study the effect of contact conditions on growth of small crack in fretting fatigue. Juoksukangas et al. [13] compared the effect of both round contact edge and the sharp contact edge on fretting fatigue behavior of a complete contact using the finely multi-axial criterion and the theory of criterion distance to calculate the cracking. In another work [14] they compared between the measured displacement from digital image correlation and the computed displacements of corresponding finite elements method, where the displacement field and its derivate were compared using the friction coefficient as a variable in the numerical model. Eugenio et al. [23] use the finite element method (FEM), the extended finite element method (XFEM) And a simple experimental to predicted crack propagation direction and path on fretting fatigue in complete contact condition. Noraphaiphipaksa et al. [15] used the maximum shear stress range criterion, the maximum relative slip amplitude and the maximum tangential stress range criterion to predict the location of fretting fatigue crack nucleation and the fretting fatigue crack path with cylindrical-on-flat contact. In addition, using the effective stress intensity factor range estimated the fretting fatigue lives. In the same year, Tongyan et al. [16] explained the effects of roughness on fretting fatigue. They indicate that the higher roughness of surface reduces the life of fretting fatigue. Rodrigo et al. [24] studied the behavior of two cables (1350-H19 aluminum) in contact; subjected to the phenomenon of fretting fatigue using a numerical method such as a 3D finite element model, they also used an experimental method on the MTS3222.21 machine. Kyvia et al. [25] published a very interesting article on aspects of fretting fatigue, based on the experiences, analyzes and research of researchers in this field. He was able to present an article to fully understand the parameters that relate to fretting fatigue such as cylindrical contact, crack nucleation, crack propagation, and fretting fatigue modeling. In this work, stress Intensity factors are calculated by the Abaqus code using the EDI calculation [22]. Fortran program allows to create a parametric mesh using the Stretching Finite Element Method SFEM [18]. This mesh permits to change various model parameters, such as the applied load, mesh sizes, the shape and the dimensions of the crack as well as the contact parameters. The problem is solved by the Abaqus computer code to determine the main crack parameter, the stress intensity factor K, and its influence on fretting fatigue behavior.

FRETTING FATIGUE CONTACT TYPE

As Fig. 1 shows, the contact types can be classified depending on the geometry of the contacting bodies [17]. The first type is plan/plan contact (Fig. 1a) or the complete contact witch a flat contact surface is used for fretting pad [17]. This type produces contact area that is independent of load. Complete contact condition necessarily has singularities at its outside edges [18], where the stress is theoretically infinite, hence, plastic deformation is expected to occur at the pad edge.

Fig. 2 presents the model utilized in this investigation; it clarifies the surface contact formed between the specimen and pad, the crack position and loads applied in two bodies. The second type is incomplete contact (Fig. 1b and 1c) where at least of the two bodies is cylinder or spherical, which produces a contact area whose size depends on the magnitude the normal force magnitude [18].
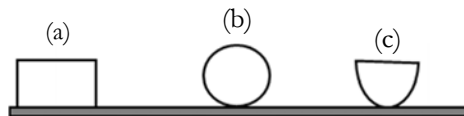

Figure 1: Different types of contacts according to the Bodies geometry: (a) plan/plan contact, (b) sphere/plan contact, c) cylinder /plan contact

The stress intensity factor is determined by considering the displacements and stress field near the crack front. It describes the stress state at crack tip. Historically, stress intensity factors K have been obtained from elastic solutions by considering 3D problems, under plain stress/strain condition.

In the case of finite dimensional structure, K_i (i = 1, 2 and 3 for mode 1, 2 and3) can be expressed in the following general form:

$$K_i = \sigma \sqrt{\pi a} \times F_i \qquad (1)$$

where F_i is the stress correction factor or form factor, taking into account the geometry of the crack as well as the type of stress applied on the structure, σ is the applied stress, and a is the crack length or the crack depth [20].
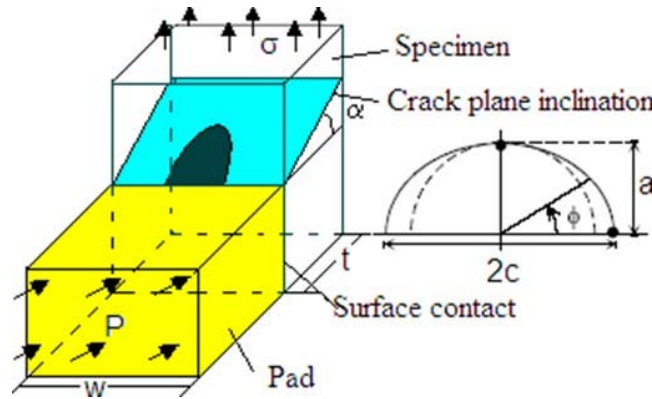

Figure 2: Specimen and pad in complete contact

EQUIVALENT DOMAIN INTEGRAL (EDI)

T he integral J is a measure of variation of potential energy, which in linear elasticity, can be directly related to the stress intensity factor SIF [21]:

$$J = \int_{\Gamma} (W dx_2 - \bar{t}_i \frac{\partial \bar{u}_j}{\partial x_1} d\Gamma) \qquad (2)$$

W is the strain energy density, Γ is the contour around the end of the crack, $\bar{u}_i$ displacement vector at a point of the contour, t_i stress vector given by $\bar{t}_i = \sigma_{ij} n_j$.

For an elastic material, this integral is identical to the rate of energy release G [19]

$$J = G_T = G_I + G_{II} + G_{III} = \frac{K_I^2}{E'} + \frac{K_{II}^2}{E'} + \frac{K_{III}^2}{2\mu} \qquad (3)$$

where:

$$E' = E \text{ in plane constraints} \qquad (4)$$

$$E' = \frac{E}{1 - \upsilon^2} \quad \text{in plane deformation} \qquad (5)$$

$$\mu = \frac{E}{2(1+\upsilon)} \quad \text{is the shear modulus} \qquad (6)$$

The Equivalent Domain Integral method use all the area A* showed in Fig.3, it is well applied to solve problems of solid in 3D with crack [18].

$$J(s) = \frac{1}{f} \iint_V \left(W - \sigma_{ij} \frac{\partial u_j}{\partial x_1} \right) \frac{\partial q(s)}{\partial x_i} dV \tag{7}$$

$$f = \int_s^{s+\Delta s} q(s) ds \tag{8}$$

q is a regularized virtual displacement of the points of A * in direction x1 between a maximum value in Γ0 and a zero minimum value in Γ1[2].
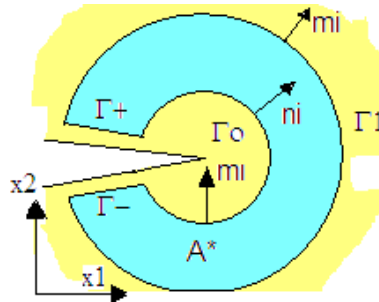

Figure 3: Definition of contours for the evaluation of the integral of equivalent domain (EDI)

STRETCHING FINITE ELEMENT METHOD (SFEM)

The finite element method by stretching of the mesh SFEM is a new method; Bentahar et al. [3] have used it for a two dimensional crack propagation. Using a Fortran program to generate a parametric mesh, this non-remeshing method allows us to stretch the mesh elements with giving new node coordinates at each new mesh. [3].
A parametric mesh is created by using a fortran Code that keeps the same number of the elements and nodes but their coordinates are changed at each new mesh parameters (mesh size, crack orientation, crack size and singularity zone size).
As Fig. 4 shows, this mesh is composed of the specimen and the pad, and they are exposed to two external forces σ and P, which means, the mesh is deformed during each new mesh parameters.
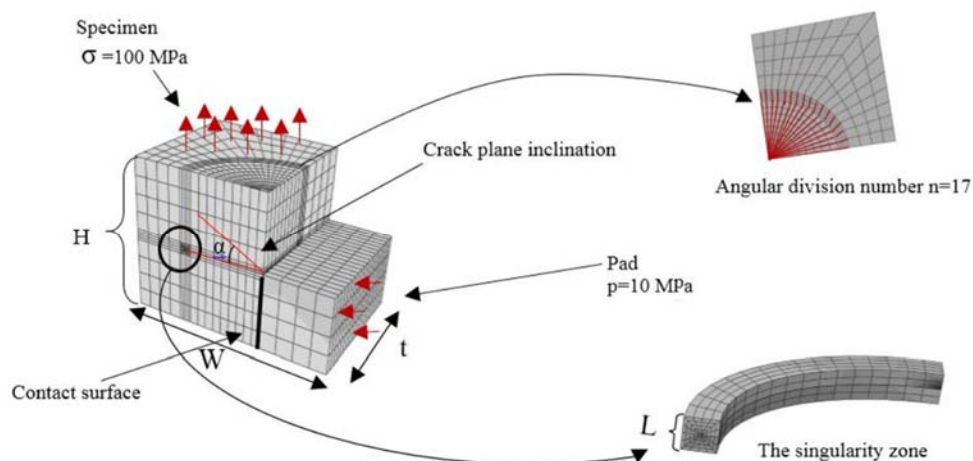

Figure 4: Mesh analysis and details of the singularity zone L, loads p and σ, and limit condition for crack plane inclination α=0°

In order to simulate the singularity that characterized the crack point, we use singular elements called 'quarter point' around the front of the crack, that is quadratic elements collapsed to obtain a triangular element.

The modeling of contact with Abaqus is based on the interaction of surfaces. The contact between the two bodies, specimen and pad is called an 'even contact' where a surface can interact on the other. A contact pair is defined by a slave surface (pad) which is the deformable surface, and the master surface (specimen) which is the most rigid surface, and the direction of contact is always perpendicular to this area. For each node of the slave surface, Abaqus looks for the nearest point on the master surface. The interaction is then discretized between the points obtained on the master surface and the nodes of the slave surface [2].

A contact pair is defined by the commands:

*CONTACT PAIR, INTERACTION=interaction-name surface-slave, surface-master [2].

NUMERICAL MODEL

A parametric mesh is composed of two bodies, which are in complete contact: the specimen that contains the crack is subjected to a tensile load σ = 100 MPa, and the pad is subjected to both a small displacement oscillation and a pressure P=10 MPa. The mesh for different sizes W/t = 1.0 with t = 25 mm. Tab. 1 shows different materials for the two bodies that are considered in the present study.

Material	Young Modulus E (GPa)	Poisson coefficient υ
Brass	92	0.33
Steel	220	0.29
Aluminum	67.5	0.34

Table 1: Material properties

For each case study, the friction coefficient parameters (f), the size of the mesh (H), the inclination of the plane (α), the size of the singularity zone (L) and the stress (σ) are varied according to Tab. 2 above:

Case study No	
f	{0.1 , 0.5, 1.0}
H (mm)	{8, 12, 16 }
α(°)	{15, 30, 45 }
L (mm)	{0.4, 0.5, 0.6}
σ (MPa)	{100, 400, 700}

Table 2: Varied mesh parameters

Due to the symmetry, only half of the structure, specimen and pad, is modeled. A fortran code is used to create a parametric mesh, which allows changing the values of the shape and dimension parameters. Abaqus 6.14 software is used to resolve the problem. The results of the stress intensity factor, for the three modes 1, 2 and 3, are obtained numerically from Abaqus.

RESULTS AND DISCUSSION

A baqus calculates the stress intensity factor for 5 contours which are shown in Fig. 5. Each contour has 17 values from the integral J=1 to J=17 according to the angular division number n. We took the stress intensity factors SIF values of the third contour avoiding the first contour because of the singularity where the stresses are infinite and the more we move away from the point of singularity, the more we lose in precision. Only the second values and third values of the contour can give good results.
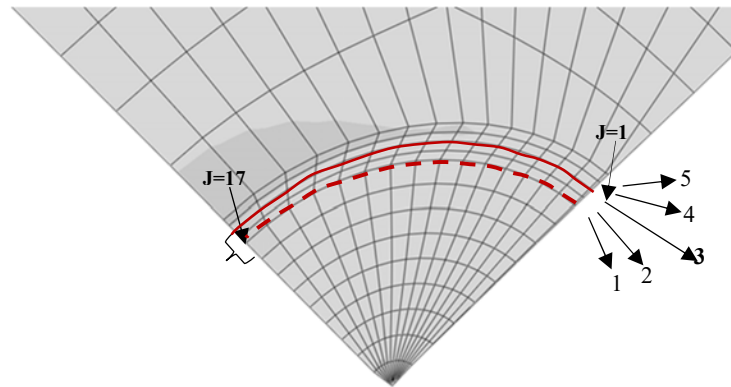
Figure 5: The position of the 5 contours.

For each contact parameter friction parameters f, mesh size H, plane inclination α, singularity zone size L, stress σ, materials steel, aluminum and brass), the results of the stress intensity factor for modes 1, 2 and 3, are represented as a function of angular division n = 17, see Fig. 7, Fig. 8, Fig. 10, Fig. 11, Fig. 12.

Fig. 6 presents a case of analysis of the mesh of a steel material with a coefficient of friction f = 1.0, a mesh of size H = 8 mm and an inclination of the crack plane α = 45 °. The same study work is used to obtain the results of the stress intensity factors according to the values of the parameters presented in Tabs. 1 and 2.
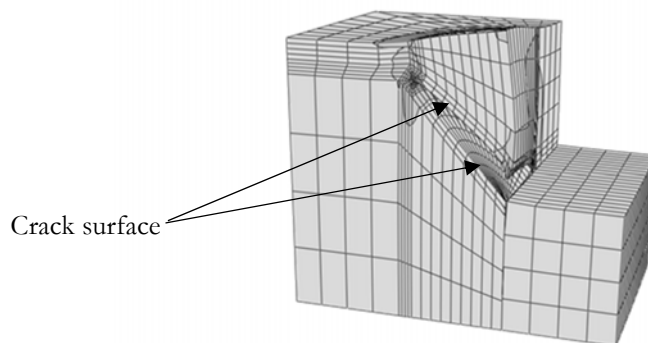

Figure 6: Mesh Analysis for f=1.0, H= 8 mm and (α=45°).

COEFFICIENT OF FRICTION

The effect of the coefficient of friction, ranging between 0.1 and 1.0 is investigated. Fig. 7 presents three graphs for three different materials, graph A for steel, graph B for aluminum and graph C for brass. For each graph, the evolution of the intensity factors of stress K_i / K_0 (Mode K1, K2 and K3) is presented as a function of the angular division n for different values of the friction coefficient.

For the three different materials, the K1 mode has the greatest value; it is the most important mode in this study because it is considered as the most damaged mode because of the tensile force applied to the mesh.

The more the coefficient of friction increase from 0.1 to 1.0, the more the value of K1 decreases. Aluminum has the greatest value of $K1 / K_0 = 20.36$ at n = 7, followed by brass with $K1/ K_0 = 20.28$ at n = 7, and steel $K1/ K_0 = 19.99$ at n = 6.

Regarding the second K_{II} mode and for each material, its evolution as a function of the number of division n increases from n=1 to n=17, but the friction effect is weaker the same observation is made for third K3 mode.

It is also observed that the value of the second mode K2 between the two points n = 1 and n = 2 is greater for aluminum and brass compared to steel. It is also noted that the first node of the zone of singularity, the value is not correct and that for the reason that this zone the constraint is infinite.
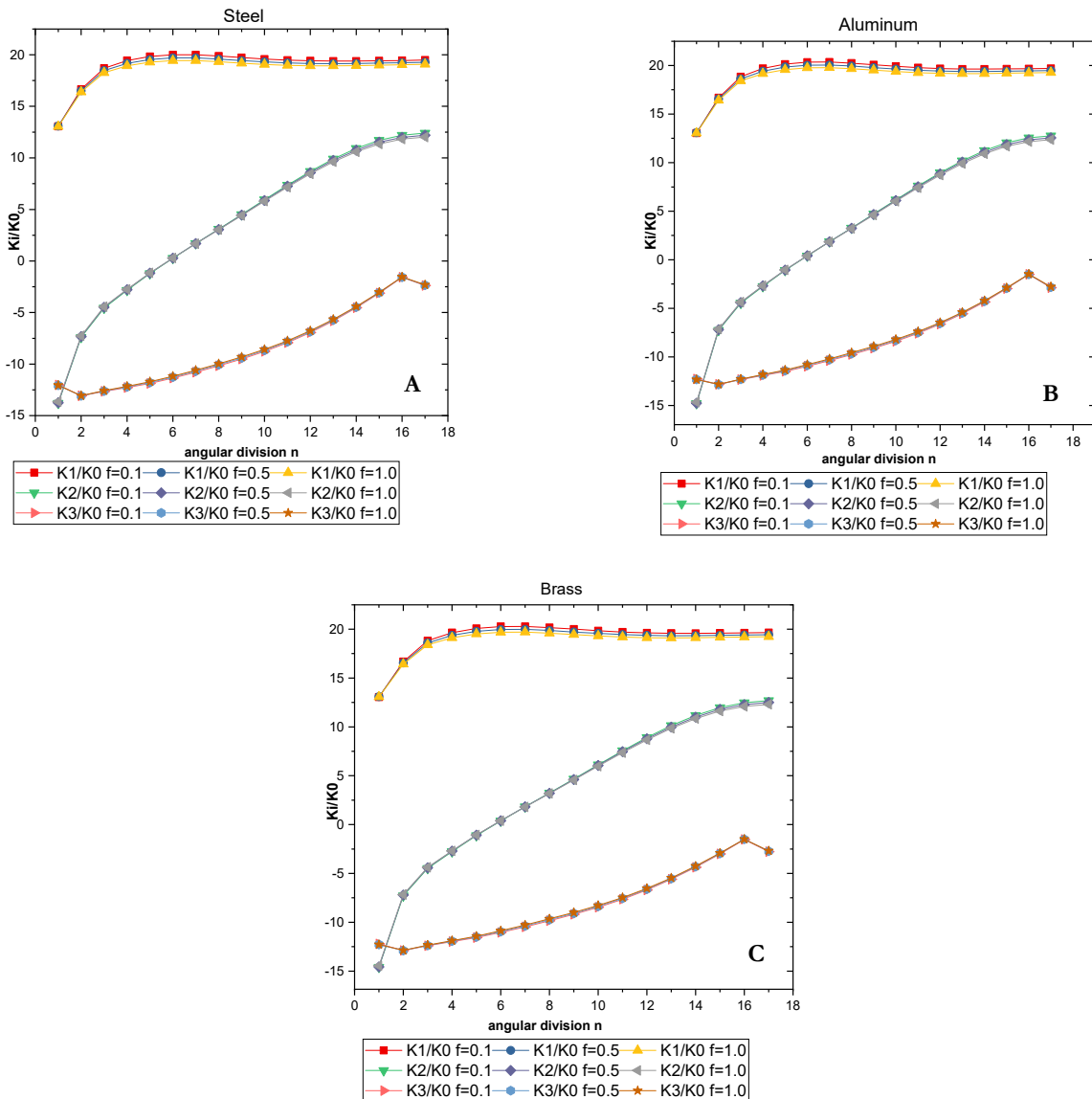
Figure 7: Factors K_i / K_0 as a function of the angular division n for different values of friction coefficient f for the three materials (A) Steel, (B) Aluminum, and (C) Brass.

EFFECT OF THE MESH SIZE

In order to identify the effect of the dimensions of the mesh on the values of the stress intensity coefficients, we varied the size mesh H of the mesh for different values H = 8, 12 and 16 mm applied to the mesh as shown in the figures below. Note that the other parameters f = 1.0, α = 15 °, L = 0.6 mm and σ = 100 MPa, remain unchanged. The results obtained from Ki / K0 are shown in the following graphs: graph A for steel, graph B for aluminum, graph C for brass. Figs. 8 presents the results of K_i / K_0 for a mesh height H as a function of the angular division number n for the three materials. Always, K1 Mode has the highest value compared to K2 and K3 Mode. The evolution of the K1 mode decreases each time the size mesh H increases. While the evolution of K2 increases as a function of the angular division number n, it is proportional to the height of the cell H, but from n=11, the proportion becomes proportional.

For the evolution of the K3 mode, it is proportional to the size mesh H. For the three tests of materials, the curves show that the values of K3 increase slightly as a function of the number of angular division n between n = 2 and n = 16. Aluminum has the highest value (K1=19.77, n = 7).
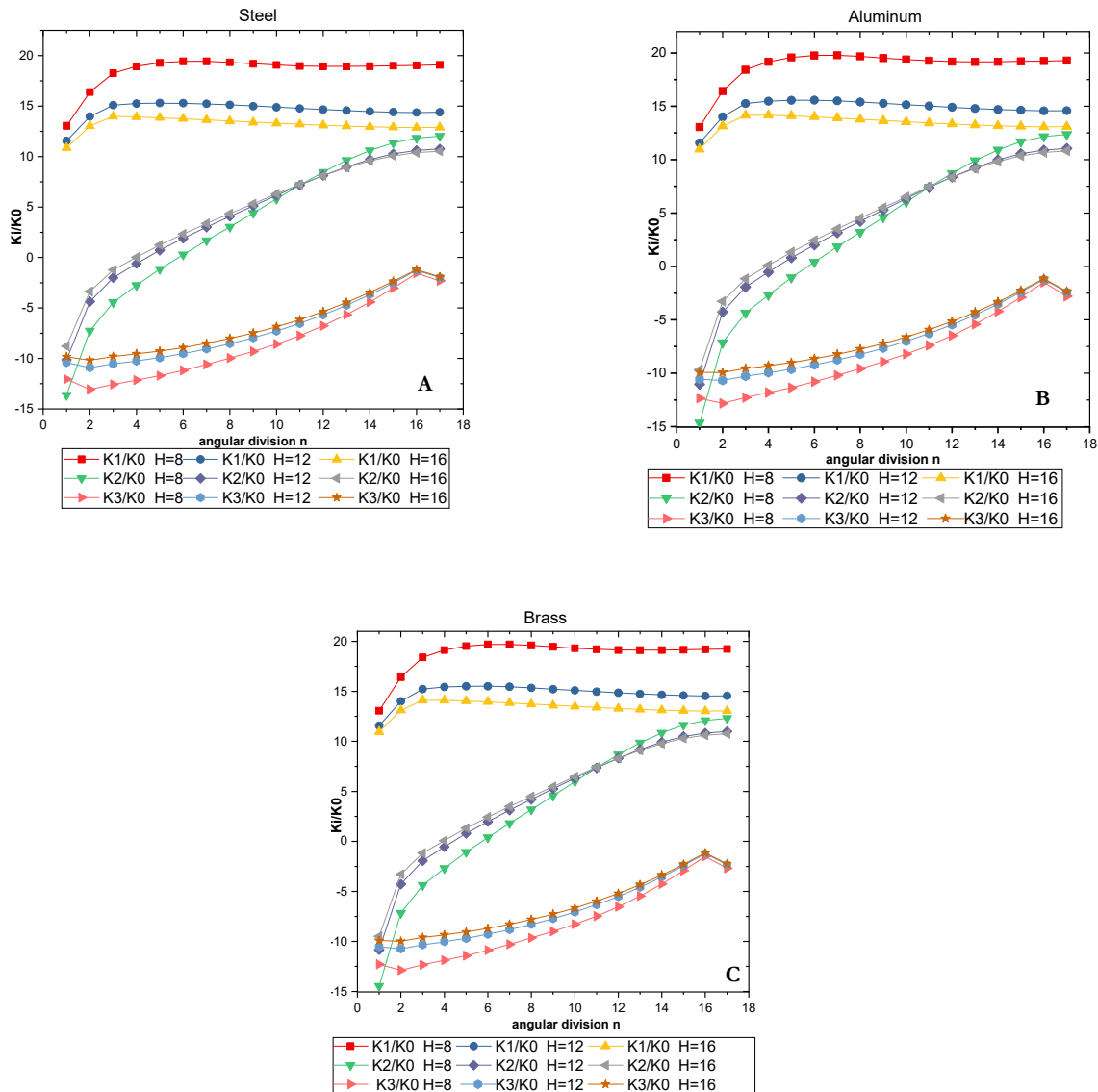

Figure 8: The factors K_i/K_0 as a function of the angular division n for different values of the mesh size (H), for the three materials (A) Steel, (B) Aluminium, and (C) Brass.

CRACK PLANE INCLINATION

The position of the crack plane has changed from the horizontal position to the tilt position of 15 °, 30 ° and 45 ° as presented in Fig. 9. For each parameter and material, the parameters H = 8 mm, f = 1.0, L = 0.6 mm and σ = 100 MPa are kept constant during the analysis. The results obtained are presented in Fig. 10.

The evolution of the crack tilt parameter is presented above in Figs. A, B and C for the steel, Aluminum and brass.

The behavior of the stress intensity factor (mode K1, K2 and K3) is similar in the graphs. In the K1 mode curve, the values increase in the first points of the angular division thereafter remain constant. On the other hand, the values of K1 are inversely proportional to the inclination of the crack plane from 15 ° to 45 °.

In the K2 mode curve, the values increase as a function of the number of angular division n, therefore we observe two parts, the first is before n = 4 or the values of K2 decrease each time the angle increases in contrast. The second part the evolution becomes proportional. The K3 mode has an inverse relationship as a function of the angle of inclination of the crack plane.

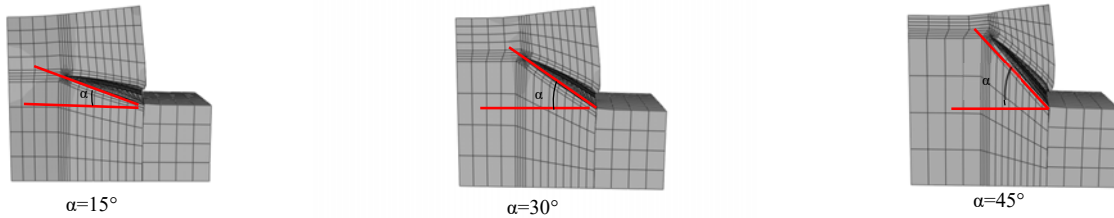Note that between the three materials aluminum has the highest value of ($K1/ K_0 = 29.30$; n=3).

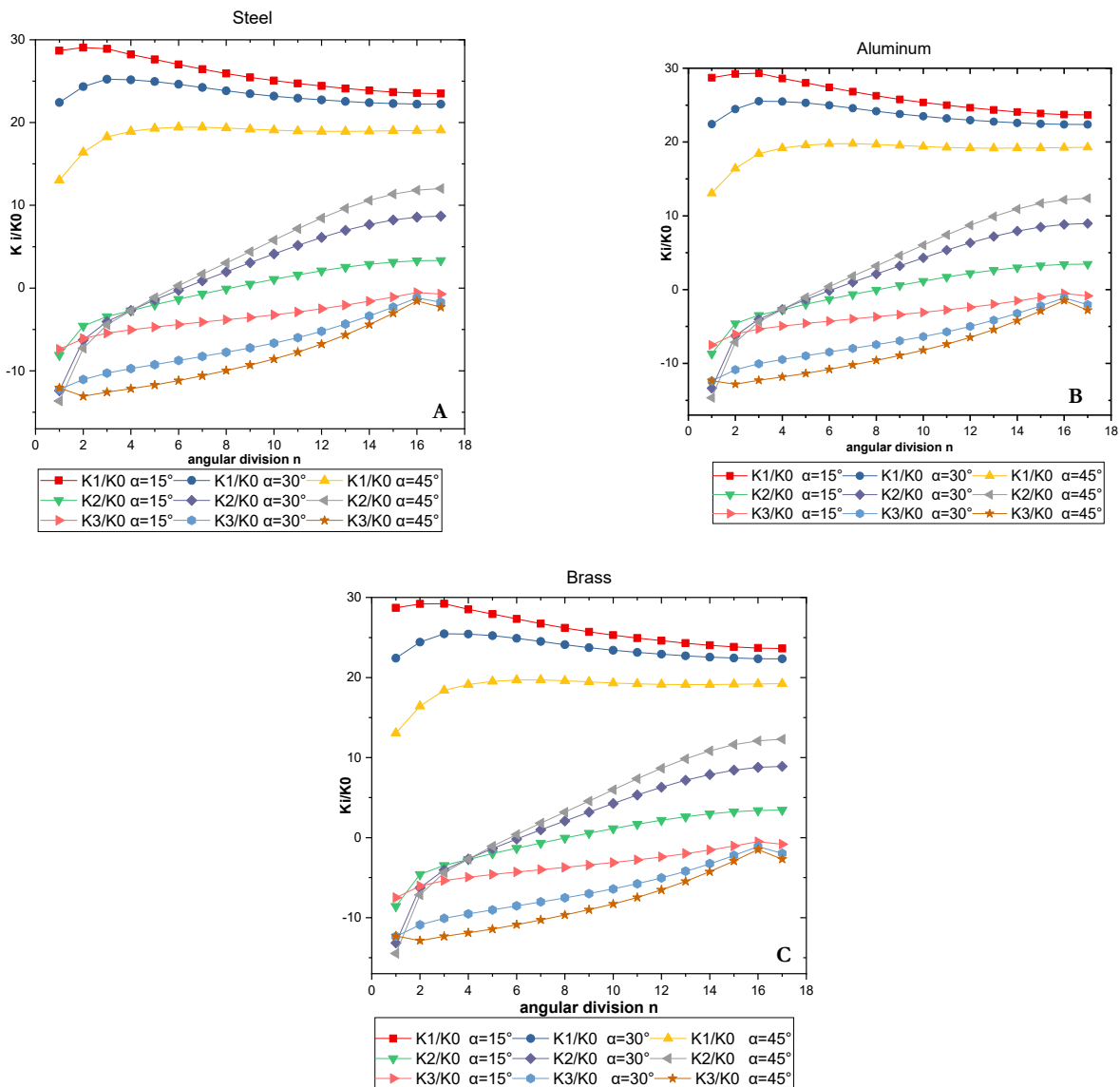Figure 9: Mesh analysis for α=15°, α=30°and α=45°.

Figure 10: Factors K_i / K_0 as a function of the angular division n for different values of crack plane inclination for the three materials (A) Steel, (B) Aluminum, and (C) Brass.

EFFECT OF THE SIDE OF THE SINGULARITY ZONE

Previous Fig. 4 presents the singular zone dimension in the mesh; this zone is located at the front of the crack. It is represented by the dimension L considered as an important parameter to study its effect on the evolution of the stress intensity factor SIF. The values of L (mm) vary as {0.4, 0.5 and 0.6} where the other parameters are fixed at H = 8 mm, f = 1.0, α = 15 ° and σ = 100 MPa. The results obtained are presented in Fig. 11 for steel, Aluminum and Brass.
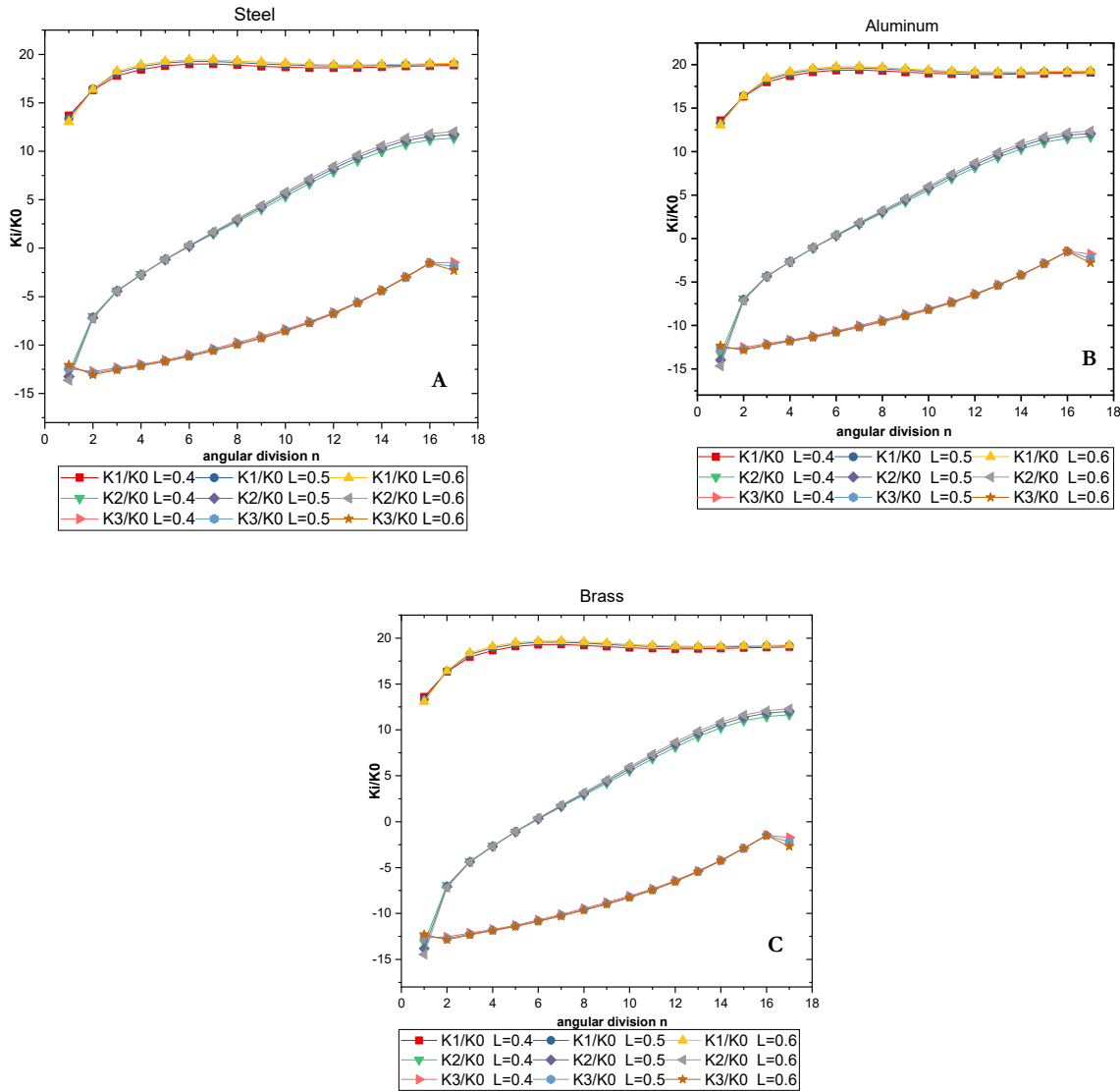

Figure 11: The factors Ki / K₀ as a function of the angular division n for different values of the side of the singularity zone L (mm) for the three materials (A) Steel, (B) Aluminum, and (C) Brass.

The results of K_i / K_0 concerning the effect of the singularity zone size L are presented in graphs A for steel, B for Aluminum and C for Brass. For each graph, the results are almost identical depending on the variation of L from 0.4 to 0.6.

The evolution of K1 mode for the three materials increases for the first points as a function of the number of angular divisions in succession, it remains constant. It is observed that the mode curve K1 for the value of L = 0.6 mm is greater than L = 0.5 mm and L = 0.4 mm. That is to say the values of SIF in the curve increase with the increase in the dimension of the singularity zone L. Note that the greatest value is recorded for aluminum ($K1 / K_0 = 19.77$ at n = 7).

The values of stress intensity factor SIF in the K2 mode curve for the three material tests increase with the angular division angle n. We also observe that the effect of the dimension of the zone of singularity L is not very visible, up to point n = 9

where its evolution increases each time L increases from 0.4 mm to 0.6 mm. For the third mode, the effect of the dimension of the singularity zone L on the evolution of K3 is very weak.

EFFECT OF THE LOAD

In this case, the effect of external forces on the evolution of the stress intensity factor SIF was studied. We always note that σ is the tensile force, and p is the pressure force of the pad on the specimen and this is the force that is created by the fretting phenomenon. This force is very small compared to the tensile force, that is why we have fixed the relation between the two forces by the following relation σ = 10 p, 10 times greater. The other parameters remain constant during the three materials tests (f = 1.0, H = 8 mm, L = 0 .6 mm and α = 45 °). The results obtained are shown in Fig. 12.
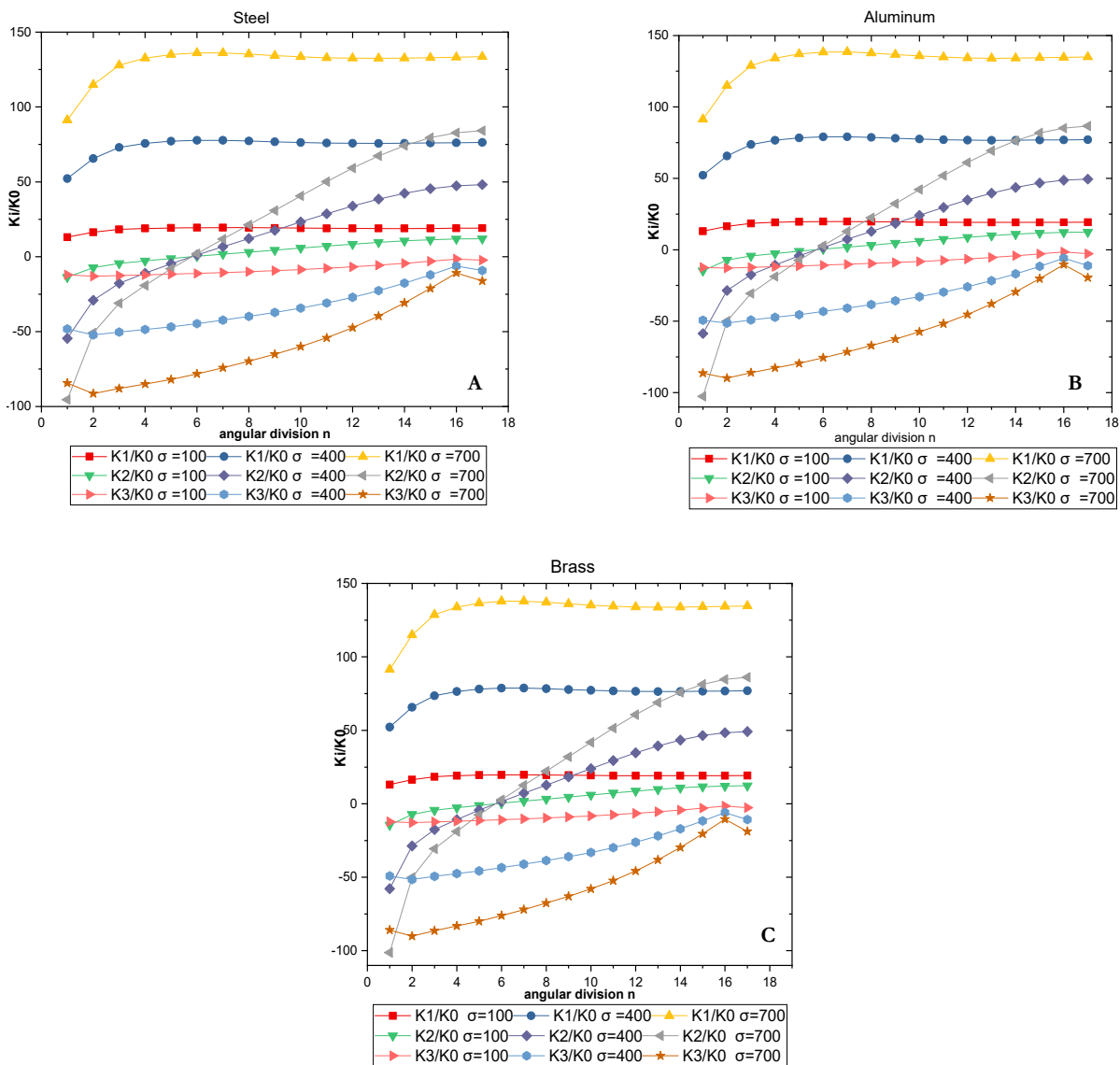

Figure 12: The factors Ki / K_0 as a function of the angular division n for different values of Load for the three materials (A) Steel, (B) Aluminum, and (C) Brass

In Fig. 12 the effect of the tensile force σ on the evolution of the stress intensity factor SIF in the three graphs appears clearly. These graphs show a proportional relationship between the change in mode K1 and the tensile force values σ for the three material
tests the highest K1 mode value appears in the aluminum graph B (K1=138.47 at n=7).
The evolution of the second mode of K2 as a function of the angular division number n is increasing. We observe two parts of the evolution on the three graphs. The first is before n = 6, where the evolution of mode K2 decreases each time the tensile force σ increase from 100 to 700 Mpa. The second part is after n = 6 , where the relation becomes inverse. For Mode K3 between n = 2 and n = 16, the evolution of the three curves increases as a function of the number of divisions n while the evolution as a function of the tensile force σ decreases each time the force σ increases by 100 at 700 MPa.

CONCLUSIONS

A numerical simulation of parametric mesh witch composed of two bodies in full contact is developed in this study. for that, a parametric mesh is analyzed with the Abaqus 6.14 software to study the effect of the different contact parameters of fretting fatigue phenomenon.
This model is subjected to two cyclic loads, the first is a tensile stress, it is applied to the specimen and the second is a perpendicular pressure on the pad. In this study, we calculated the stress intensity factor in three modes K1, K2 and K3.
The results are presented on graphs, which show the evolution of the factors as a function of the angle of division n for the different parameters.
From the results obtained, the parameters are divided into two groups. The first group (the size mesh H, the angle of inclination of the plane of crack α and the tensile force σ) all have a significant effect on the evolution of the stress intensity factor SIF, and the second group (coefficient of friction and the dimension of the singularity zone L) have a weaker effect.
Through the results obtained, K1 mode shows the higher value for the three material tests and for all different parameters.
It is noted that the following parameters: the size mesh H, the inclination of plane of the crack α and the coefficient of friction have an inverse effect on the evolution of mode K1.
Regarding the material effect, although the results obtained for the three material tests are close, Aluminum is more influential on the evolution of K1 mode.
We conclude that the parameters which have been applied externally (σ, H and, α) have an efficiency compared to the parameters which have been applied internally (f, L and the different materials).
Finally, with this SFEM method we can study a large field (range) of parameters and compare several results at the same time which allows us to make a rather rich study.

REFERENCES

[1] Maslan, M.H., Sheikh, M.A., Arun, S. (2014). Prediction of Fatigue Crack Initiation in Complete Contact Fretting Fatigue Applied Mechanics and Materials Vol. 467. pp 431-437, Trans Tech Publications, Switzerland.
DOI: 10.4028/www.scientific.net/AMM.467.431
[2] Benzaama, H. (2008), Study and modeling in 3-dimensional finite element and Fretting fatigue application, PhD thesis, University of Scence and Technologie of Oran, M.B. Algeria
[3] Bentahar, M., Benzaama, H., Bentoumi, M., Mokhtari, M. (2017). A New Automated stretching finite element method for crack propagation in two dimension Journal of theoretical and applied mechanics, 55, 33.
DOI: 10.15632/jtam-pl.55.3.869.
[4] Hojjati Talemi, R., Abdel Wahab, M., De Baets, P. (2011), Numerical modelling of fretting fatigue, Journal of Physics: Conference Series, 305(1), St Anne's College, University of Oxford, 9th International Conference on Damage Assessment of Structures (DAMAS 2011).
[5] Lehtovaara, A., Lönnqvist, C., & Mäntylä, A. (2010). A numerical model for the calculation of fretting fatigue crack initiation for a smooth line contact. Tribologia - Finnish Journal of Tribology, 29(1), 7-16.
https://journal.fi/tribologia/article/view/69634.
[6] Nowell, D. (1988), An Analysis of Fretting Fatigue, PhD thesis, University of Oxford.
[7] Ochi, Y., Hayshi, H., Tateno, B., Ishii, A. and Kuroki, T. (1996), Effects Of Contact Pressure and Slip Amplitude On Fretting Fatigue Properties Of Rail Steel With Fish Plate, Transactions on Engineering Sciences, 13, pp 6.
DOI: 10.2495/LD960761.

[8] Venkatesh, T.A., Conner, B.P., Suresh, S. et al. (2001). An experimental investigation of fretting fatigue in Ti-6Al-4V: the role of contact conditions and microstructure. Metall and Mat Trans A 32, 1131–1146. DOI: 10.1007/s11661-001-0124-8.

[9] Kondo, Y., Sakae, C., Kubota, M., Nagasue, T. (2004), Fretting fatigue limit as a short crack problem at the edge of contact ,Journal of Fatigue and Fracture of Engineering Materials and Structures, 27(5), pp 361-368. DOI: 10.1111/j.1460-2695.2004.00750.x.

[10] Ciavarella, M., Demelio, G. and Hills D.A. (2008), Fretting Fatigue Problems Associated With Almost Flat Contacts.

[11] Heung soo, K., Mall, S., Ghoshal, A. (2010). Two-Dimensional and Three-Dimensional Finite Element Analysis of Finite Contact Width on Fretting Fatigue, Materials Transactions, 52(2), pp. 147-154. DOI: 10.2320/matertrans.M2010268.

[12] Kataoka, S, Ono, H, Kubota, M & Kondo, Y. (2012). Effect of contact conditions on growth of small crack in fretting fatigue, Nihon Kikai Gakkai Ronbunshu, A Hen/Transactions of the Japan Society of Mechanical Engineers, Part A, 78(785), pp. 1-13. DOI: https://doi.org/10.1299/kikaia.78.1.

[13] Juoksukangas, J., Lehtovaara, A., Mäntylä, A. (2013). The effect of contact edge geometry on fretting fatigue behavior in complete contacts, Wear, 308(1–2), 206–212. DOI: 10.1016/j.wear.2013.06.013.

[14] Juoksukangas, J., Lehtovaara, A. and Mäntylä, A. (2016). A comparison of relative displacement fields between numerical predictions and experimental results in fretting contact, Proc. IMechE, Part J: J. Engineering Tribology, 230(10), 1273–1287. DOI: 10.1177/1350650116633573

[15] Noraphaiphipaksa, N., Manonukul, A., Kanchanomai, C. (2017). Fretting Fatigue with Cylindrical-On-Flat Contact:Crack Nucleation, Crack Path and Fatigue Life, Materials, 10, 155, DOI:10.3390/ma10020155.

[16] Yue, T., Abdel Wahab, M. (2017), Roughness Effects on Fretting Fatigue, IOP Conf. Series: Journal of Physics: Conf. Series 843 (2017) 012056, Porto, Portugal, 6th International Conference on Fracture Fatigue and Wear.

[17] Haidir Maslan, M. (2015), Development of predictive finite element models for complete contact fretting fatigue , PhD thesis, the Faculty of Engineering and Physical Sciences, School of Mechanical, Aerospace and Civil Engineering, University of Manchester.

[18] Benzaama, H., Giner, E., Elachachi, B. (2007). A 3D finite element modelling of semi-elliptical inclined cracks under fretting fatigue conditions, Proceeding of the international conférence on modeling and simulation. Algiers, Algeria.

[19] Saidi, H. Ouled Ahmed, M. (2006), Calculation of the stress intensity factor by abaqus for a central crack and an emerging crack, master thesis, University Saad Dahlab Blida, Algeria.

[20] Delvallee, I. (1999). Harmfulness of a semi-elliptical defect of complex orientation in a closed cylindrical shell subjected to internal pressure, Phd thesis, University Of Science And Technology Of Lille 1, UFR of mathematics. https://ori-nuxeo.univ-lille1.fr/nuxeo/site/esupversions/d07db432-cc59-457d-ac18-20077598a6c2

[21] Lalonde, S. (2008). Modeling of crack propagation in Gears by the boundary element method, master in mechanical engineering thesis, Higher Technology School, Montérial https://espace.etsmtl.ca/id/eprint/108/4/LALONDE_S%C3%A9bastien-web.pdf

[22] Shivakumar, K. N. and Raju, I. S. (1992), An equivalent domain integral method for three-dimensional mixed-mode fracture problems, Engineering Fracture Mechanics, 42(6), pp. 935-959. DOI:10.1016/0013-7944(92)90134-Z

[23] Giner, E., Díaz-Álvarez, J., Marco, M., Miguélez, M.H., (2015). Orientation of propagating crack paths emanating from fretting-fatigue contact problems. Frat. Ed Integrità Strutt. 10, 285–294. DOI: 10.3221/IGF-ESIS.35.33.

[24] Pereira, R.L., Díaz, J.I.M., Ferreira, J.L.A., da Silva, C.R.M., Araújo, J.A. (2020). Numerical and experimental analysis of fretting fatigue performance of the 1350-H19 aluminum alloy. J. Braz. Soc. Mech. Sci. Eng. 42, 419. DOI: 10.1007/s40430-020-02498-w

[25] Pereira, K., V. Vanegas-Useche, L., Abdel Wahab, M., 2020. Aspects of Fretting Fatigue Finite Element Modelling. Comput. Mater. Contin. 64, 97–144. DOI: 10.32604/cmc.2020.09862